Acta Technica 62, No. 3B/2017, 667–680

Ultimate shear bearing capacity analysis of fibrous concrete wall[1]

Yuanyuan Zhao[2], Quan Yuan[2], Peng Chang[2]

Abstract. Based on the theoretical analysis and experimental research, the composite materials equivalent elastic plate model of fibrous concrete wall was developed by incorporating the mechanical characteristics, failure process and failure mode of the fibrous concrete wall. The twin shear unified strength theory is applied to derive the ultimate shear bearing capacity formula of the fibrous concrete wall and analyze the preliminary research walls apply this formula. The theoretical results are compared with the experimental data, the result show that the model can better reflect the ultimate bearing capacity properties of the ecological composite wall, which can be applied to check the ultimate shear bearing capacity under different sizes, reinforced and filled materials of the ecological composite wall.

Key words. Fibrous concrete wall, ultimate bearing capacity, twin shear unified strength theory.

1. Introduction

Being a traditional industry on the extensive scale in China, residential construction maintains the way of coarse production. There lie several problems such as the simple form of residential construction, poor aseismic performance, lower consumption of new building material, etc. Therefore, the new direction in Chinese residential development is to develop the new residential construction systems with the low weight, energy-saving, good aseismic performance, economy and environmental protection.

Fibrous concrete wall, shown in Fig. 1, was a new type of composite wall setting of bearing, maintenance and insulation. Compared with the traditional structure, this new composite wall was much lighter, thinner, faster and conducive to the residential system industrialization.

The ecological composite wall structure is mainly constructed with the pre-cast

[1]The authors gratefully acknowledge the financial support provided by the National Natural Science Foundation of China (51508021).

[2]Beijing Jiaotong University, Beijing 100044, China

fibrous concrete wall, concealed frame and floor by means of assembling and casting. As one of the main bearing components, the fibrous concrete wall is consisted by two parts, a concealed frame and a fibrous concrete wall. Linking and restraining the fibrous concrete wall, the concealed frame is composed of end frame columns and concealed beams. The fibrous concrete wall is prefabricated with reinforced concrete frame grids and filler blocks. The beams and columns of reinforced concrete frame grids, called ribbed beams and ribbed columns, are small in section and reinforcement as shown in Fig. 2.

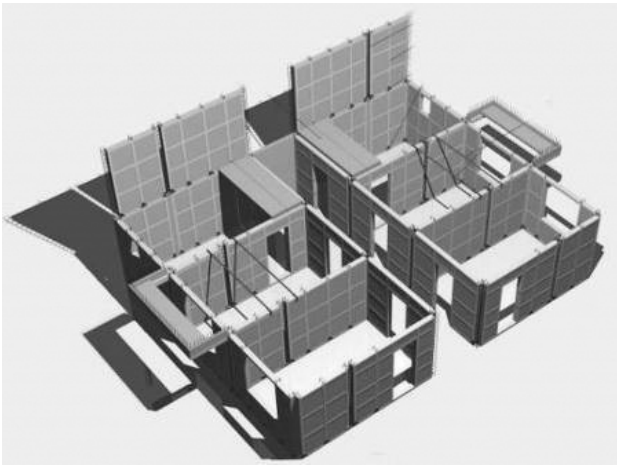

Fig. 1. Fibrous concrete wall structure system.

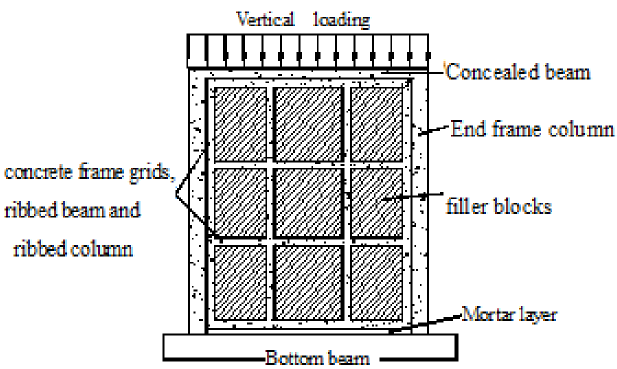

Fig. 2. Fibrous concrete wall.

As the main bearing member of the structural system, the fibrous concrete wall often fails in shear under vertical and horizontal loads. Ultimate bearing capacity analysis of the wall [1]–[4] becomes the key concern of the ultimate bearing capacity of the structural analysis and seismic performance evaluation. The shear resistance organization is given at capacity limit state by considering the wall with the force characteristics, the failure process and failure mode. According to the previous experimental studies and theoretical analysis, the fibrous concrete wall equivalent elastic plate inclined strut simplified calculation model is developed and the ultimate bearing capacity calculating formula of fibrous concrete wall based on the twin shear unified strength theory is established. Furthermore, the numerical results are compared with the experimental results.

2. Test review

2.1. The failure modes of the wall

In earthquake, the fibrous concrete wall is always in the complicated force-state, which is pressed by bending, shearing, and compression. This paper indicates that the possible ultimate failure modes of the wall can be classified into the shearing failure mode and the bending failure mode.

2.1.1. Shearing failure mode In the elastic stage, as a whole load-bearing member, the wall's load-bearing performance is different from that of the concrete elastic slab the block slab, since the concrete frame is composed of ribbed beams, ribbed columns and concealed frame coordinates with the filler blocks. Generally, the wall can be treated as an equivalent elastic composite slab. In the elastic-plastic stage and failure stage, the filler blocks in the wall undergo the process from faint cracks to serious crush and spalling. Finally, the wall degrades to the pure frame only composed by concrete frame grids and concealed frame. The ribbed columns and concealed frame have no evident damage, but there are many shearing plastic hinges on the ribbed beams. The shearing failure is the main failure mode of the wall, whose load-bearing members such as filler blocks, concrete frame grids and concealed frame can play a key role one by one during the elastic stage, the elastic-plastic stage and failure stage successively, so the shearing failure of the wall makes the structure in possession of several aseismic defending lines and is considered as a reasonable failure mode shown in Fig. 3.

2.1.2. Bending failure mode The wall sometimes suffers the bigger integral bending moment, which causes the end frame columns at the close side and distant side to endure heavy axial compression and tension, respectively. If the wall is designed in the wrong way, the integral anti-bending strength of wall will be insufficient, and the concrete compressive or tensile destroy will be found at the feet of the end frame columns before the damage of the inner fibrous concrete wall. This kind of damage will lead to the total failure of structure directly, in other words, it can't form a reasonable failure mechanism, which can be observed in Fig. 4.

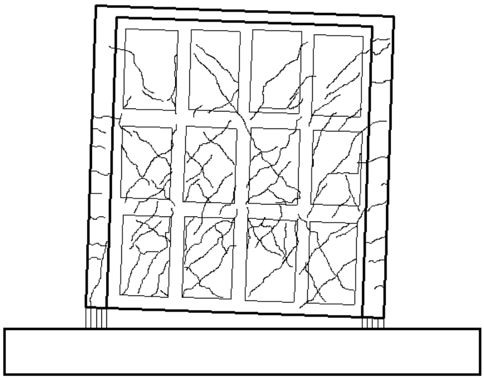

Fig. 3. Bending failure mode of the wall

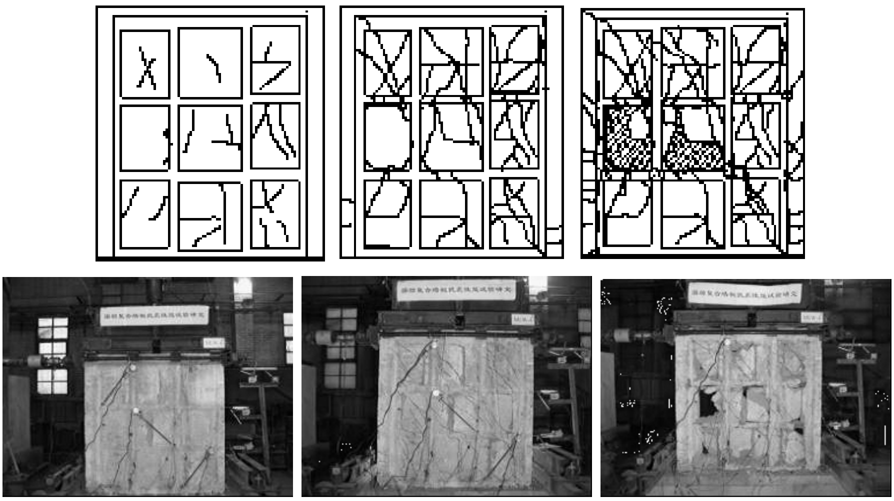

Fig. 4. Failure process of walls: from the left to the right elastic stage, elastic-plastic stage, failure stage.

2.2. The load-bearing characteristics of the wall

According to the previous study [5], the shearing failure process of most walls can be classified into three stages, namely elastic stage, elastic-plastic stage and failure stage, which are shown in Fig. 4. In the elastic stage, the wall is a whole the force components, the frame grid which are consisted of ribbed beam and ribbed column deform coordination with filled block. In the elastic-plastic stage, with the increase of the horizontal load, the cracks increase in the filled block and are extended to the ribbed beam and ribbed column. In the failure stage, some diagonal cracks are extended through to the box column in the ribbed beam and ribbed column, gradually the dispersion inclined cracks are formed in the wall along the diagonal direction where the wall is divided into a number of diagonal strut, but it can still bear the vertical loads, and has good anti-collapse capabilities.

The main load-bearing characteristics of the wall can be concluded as follows:

1. The concealed frame composed of end frame columns (connecting column) and concealed beam links and restrains the fibrous concrete wall to be the main load-bearing member of the wall. The filler blocks, the ribbed beams and ribbed columns are contacted while the wall is subjected to the horizontal loading. The concrete frame grids and the filler blocks affect mutually and utilize their performance respectively while the wall is bearing horizontal loading. On one hand, the concrete frame grids confines the filler blocks; on the other hand, the concrete frame grids are reacted by the blocks. At the same time, the cast-in-place wall enables the deformation of the concealed frame and the fibrous concrete wall to be concordant.

2. As the filler blocks are restricted by the concrete frame grids, cracks are limited in a certain range. Under the action of cyclic loading, the cracks trend to close when the wall is loaded reversely. So, the fibrous concrete composite wall can bear loading continuously and effectively. In addition, the lateral force resisting rigidity can be enhanced. At the same time, the cracks and the inelastic deformation of the filler blocks can absorb a large amount of the earthquake energy actively and improve ductility of the structure effectively, which resembles an energy dissipation device.

3. The unique structural character of the wall ensures that three-part members of the bearing capacity system (i.e. filler blocks, concrete frame grids and concealed frame) can play a key role gradationally in three stages (i.e. elastic stage, elastic-plastic stage and failure stage), which makes the structure in possession of several aseismic defending lines .Accordingly, different load-bearing models should be chosen during different periods in the test.

3. Overview of the twin shear unified strength theory

Yu [6]–[8] established the twin shear unified strength theory by considering the stresses in the cell body and their different effects on the material yield. Twin shear unified strength theory shows that when influence functions of the two large shear stress and normal stress acting on the cell body reach a certain extreme, the material damage begins to occur. His strength theory is given by

$$F = \left(\sigma_0 + \frac{1+b-\alpha}{2\alpha}\right)^2 + \frac{(1+b+\alpha)^2}{\alpha\,(1+b)}\tau_0^2 = \frac{(1+\alpha+b)^2}{4\alpha^2}\,,$$

$$|\tau_0| \geq |\sigma_0|\,\frac{\sqrt{\alpha}}{1-\alpha}\,, \tag{1}$$

$$F' = \left(\sigma_0 + \frac{1-\alpha-\alpha b}{2\alpha}\right)^2 - \frac{(1+b+\alpha)^2}{\alpha(1+b)}\tau_0^2 = \frac{(1+\alpha+\alpha b)^2}{4\alpha^2}\,,$$

$$|\tau_0| \le |\sigma_0| \frac{\sqrt{\alpha}}{1-\alpha}\,, \tag{2}$$

where σ_1, σ_2 and σ_3 are normal stress, respectively; $\alpha = f_\mathrm{t}/f_\mathrm{c}$ is the ratio of the tension strength and compression strength for the material; f_t and f_c are the uniaxial tensile strength and the uniaxial compressive strength of the material, respectively; b reflects the intermediate normal shear stress and corresponding surface of the normal stress on the material damage parameters.

4. Ultimate bearing capacity analysis of the fibrous concrete wall

The experiment results show that the fibrous concrete wall goes through the shearing damage in three stages. In the elastic stage, fibrous concrete wall is a whole force component, the frame grid consisted of ribbed beam and ribbed column deforms the coordination with filled block. The mechanical properties are different from the concrete elastic plate and light block. On the macro level, which can be regarded as the composite material equivalent elastic plate [9] with the block matrix and reinforced fiber of the concrete ribbed beam, ribbed columns, work principle between end frame and the equivalent elastic plate is similar to interaction constraint between grid and block, therefore the equivalent elastic composite plates is equivalent to oblique strut and to establish the overall diagonal strut model is a simple and practical macro calculation model, which is shown in Fig. 5.

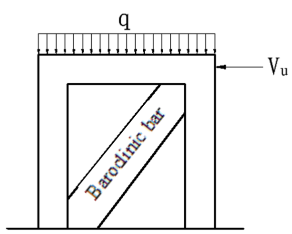

Fig. 5. Calculation model of composite wall.

4.1. Tensile strength of composites

Figure 4 presents the pore pressure development measurements of plain SCC and mono-fiber reinforced SCC at different depths. It can be observed that the maximum pore pressures measured in plain SCC at all depths are much higher than those of fiber reinforced SCC. The times at maximum pore pressure of fiber reinforced SCC at all depths are longer than that of plain SCC. Micro PP fiber plays a more significant role in reducing pore pressure than macro PP fiber and steel fiber. For all series, the pore pressure in 30 mm depth is the highest. Comparing Fig. 4c and other figures, it clearly shows that the addition of steel fiber plays some roles in pore pressure reduction in deeper regions of SCC exposed to fire. This observation is also confirmed by M. R. Bangi in his latest research paper. Macro PP fiber is used more and more widely in concrete construction, therefore, its fire resistance is concerned gradually. From Fig. 4d, it can be seen that macro PP fiber plays a more efficient role in pore pressure reduction than steel fiber. Comparing macro PP fiber with steel fiber and micro PP fiber, it seems that the addition of macro PP fiber has a better effect in shallow regions than in deep regions during fire exposure. This is likely a result of the geometric size of macro PP fiber.

Figure 6 presents the calculation method of the tensile strength of composite equivalent elastic plate by taking the representative volume element [10] in the fibrous concrete wall.

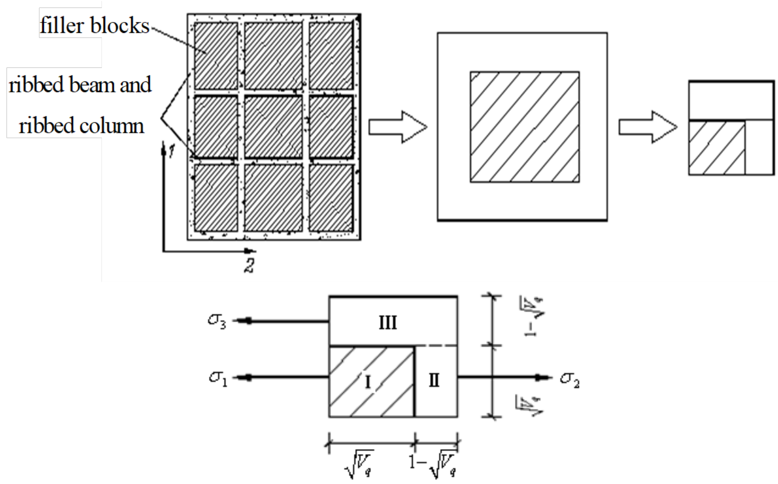

Fig. 6. Representative volume element of composite wall.

Assume the block and concrete fiber deformed coordinate in the horizontal force, we have

$$\Delta_{\mathrm{q}} + \Delta_{\mathrm{co}} = \Delta_{\mathrm{c}}\,. \tag{3}$$

Where the subscript q, co and c are the block, concrete and fibrous material, respectively. Geometric equation

$$\varepsilon_{\mathrm{q}} \cdot \sqrt{V_{\mathrm{q}}} + \varepsilon_{\mathrm{co}} \cdot \left(1 - \sqrt{V_{\mathrm{q}}}\right) = \varepsilon_{\mathrm{c}}\,. \tag{4}$$

The Hooke's law, $\varepsilon = \sigma/E$, substitution of the material tensile strength f_{t} for σ, that is substitution $\varepsilon = f_{\mathrm{t}}/E$ into equation (4)

$$\frac{f_{\mathrm{tq}}}{E_{\mathrm{q}}} \cdot \sqrt{V_{\mathrm{q}}} + \frac{f_{\mathrm{tco}}}{E_{\mathrm{co}}} \cdot \left(1 - \sqrt{V_{\mathrm{q}}}\right) = \frac{f_{\mathrm{tc}}}{E_{\mathrm{c}}}\,. \tag{5}$$

The tensile strength of composite can be obtained as follow:

$$f_{\mathrm{tc}} = f_{\mathrm{tq}} \cdot \frac{E_{\mathrm{c}}}{E_{\mathrm{q}}} \cdot \sqrt{V_{\mathrm{q}}} + f_{\mathrm{tco}} \cdot \frac{E_{\mathrm{c}}}{E_{\mathrm{co}}} \cdot \left(1 - \sqrt{V_{\mathrm{q}}}\right) , \tag{6}$$

where E_{c} is the elastic modulus of composite materials [11], E_{q} is the elastic modulus of the matrix [12], V_{q} is the matrix volume fraction.

4.2. Shear ultimate strength analysis of fibrous concrete wall based on the unified strength theory

4.2.1. Basic assumptions According to the pre-trial observation and analysis, the wall cracks increased significantly with the displacement continues to increase when the wall is destroyed stage, the cracks increased and wider, and ultimately the wall formed through the inclined cracks along the diagonal direction, the angle materials was destroyed in the joint action of compressive stress and shear stress, and capacity began to decline. Based on the above research, we propose the following assumptions [13], [14]:

1. Fibrous concrete wall using the overall diagonal strut model.
2. Framework node of the inclined struts end always appear plastic hinge before reaching ultimate bearing capacity, and the framework node in the moment of ultimate is given as

$$M_{\mathrm{A}} = M_q mri \,, \tag{7}$$

   where M_{A} is bending force of node A, M_{i} is the smaller of ultimate moment between the frame columns and frame beams.

3. Frame members act the axial force and bending moment while reaching the ultimate of capacity, it should not directly take the limit bending moment while calculating the contact length of the equivalent elastic plate, the bending moment at the plastic hinge should be taken as

$$M_{\mathrm{M}} = \lambda_{\mathrm{c}} M_{\mathrm{uc}},\ M_{\mathrm{N}} = \lambda_{\mathrm{b}} M_{\mathrm{ub}} \,, \tag{8}$$

   where: M_{M} and M_{N} are the moment of frame columns and frame beam at the plastic hinge, respectively; λ_{c} and λ_{b} are the moment bending reduction factor of frame columns and frame beam, respectively. In the present analysis, the reduction factor is assumed as 0.6.

4.2.2. Shear ultimate strength analysis of fibrous concrete wall Based on the above assumption, combined with experimental research of the fibrous concrete wall and the experimental study and analysis is related to the corner working condition of filled frame Saneinejad[15] to analysis the frame beam and frame column mechanical properties of fibrous concrete wall. It is assumed that when the fibrous concrete wall is in the elastic-plastic stage, compressive stress and shear stress distribute uniformly in the pressure angle region of the contact surface, shear stress is zero at the plastic hinge, as shown in Figure 7.

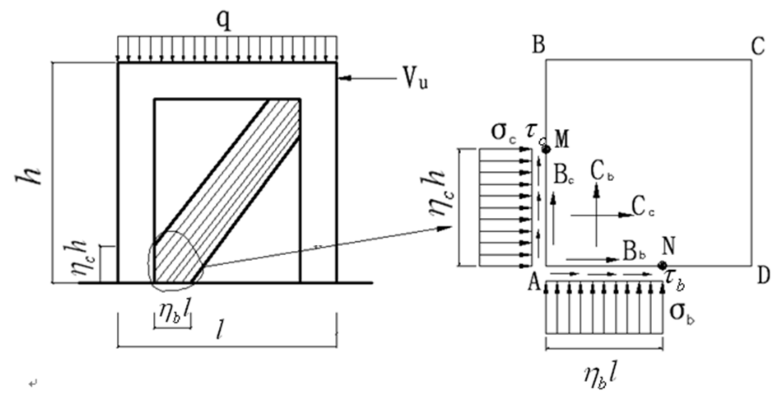

Fig. 7. Stress distribution at the corner.

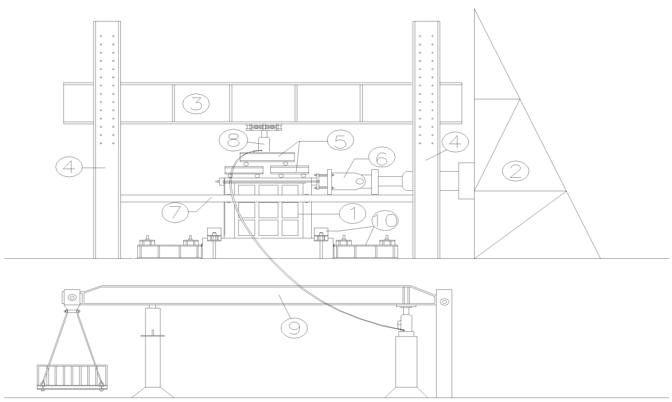

Fig. 8. Experimental set-up: 1-Test specimen, 2-Reaction wall, 3-Steel beam, 4-Steel column, 5-Distributive girder 1&2, 6-Actuator, 7-Lateral support, 8-Jack, 9-Load voltage stabilizer, 10-Fixing beam 1&2.

Take part mechanical analysis, the force balance can be obtained as

$$V = C_{\rm c} + B_{\rm b}\,, \tag{9}$$

$$\left\{\begin{array}{ll} C_{\rm c} = \sigma_{\rm c}\eta_{\rm c}ht & C_{\rm b} = \sigma_{\rm b}\eta_{\rm b}lt \\ B_{\rm c} = \tau_{\rm c}\eta_{\rm c}ht & B_{\rm b} = \tau_{\rm b}\eta_{\rm b}lt \end{array}\right. , \tag{10}$$

where the contact length of the beam and column are $\eta_{\rm b}l$ and $\eta_{\rm c}h$, respectively; $\eta_{\rm c}$

and η_{b} are the effective contact length factor of the contact surface between the frame columns and beams and the equivalent elastic plate, respectively; l and h are the width and height of the frame, respectively; σ_{c} and σ_{b} are the equivalent normal stress of the contact surface, respectively; τ_{c} and τ_{b} are equivalent shear stress of the contact surface, respectively; C_{c}, C_{b}, B_{c} and B_{b} are the positive pressure and shear of the columns and beams, respectively; t is the wall thickness.

The pressure angle material is damage under the effect of normal stress and shear stress while the load reached ultimate. Yu [16] proposed a framework normal stress and shear stress relationship combined with Saneinejad model [15] and test rules of the fibrous concrete wall. It can be written as

$$\tau_{\mathrm{c}} = \xi \sigma_{\mathrm{c}} k,\ \tau_{\mathrm{b}} = \xi \sigma_{\mathrm{b}} / k\,, \tag{11}$$

where ξ is the friction coefficient between equivalent elastic plate and frame; k is the ratio of height to width of the frame, $k = h/l$.

The equivalent stress which is contact surface between equivalent elastic plate and frame columns, beams is denoted by σ_{c}, σ_{b}, AM and AN were taken from the body segment, taking moment for the A-point and the balance equation are obtained as following

$$\begin{cases} \eta_{\mathrm{c}} h \cdot \sigma_{\mathrm{c}} \cdot t \cdot 0.5 \cdot \eta_{\mathrm{c}} h = M_{\mathrm{A}} + M_{\mathrm{M}} \\ \eta_{\mathrm{b}} l \cdot \sigma_{\mathrm{b}} \cdot t \cdot 0.5 \cdot \eta_{\mathrm{b}} l = M_{\mathrm{A}} + M_{\mathrm{N}} \end{cases}, \tag{12}$$

where M_{A} is the bending moment of A-point, M_{M} and M_{N} are the bending moments at plastic hinge of the framework columns and framework beam, respectively.

When the equivalent normal stress reaches its maximum value σ_{c0} andσ_{b0}, that is to say the plastic hinge appears, then Eq. (12) becomes

$$\begin{cases} \eta_{\mathrm{c}} h \cdot \sigma_{\mathrm{c0}} \cdot t \cdot 0.5 \cdot \eta_{\mathrm{c}} h = M_{\mathrm{i}} + \lambda_{\mathrm{c}} M_{\mathrm{uc}} \\ \eta_{\mathrm{b}} l \cdot \sigma_{\mathrm{b0}} \cdot t \cdot 0.5 \cdot \eta_{\mathrm{b}} l = M_{\mathrm{i}} + \lambda_{\mathrm{b}} M_{\mathrm{ub}} \end{cases}. \tag{13}$$

Substituting Eq. (8) into Eq. (**??**), we can obtain an effective length factor of the contact area

$$\begin{cases} \eta_{\mathrm{c}} = \sqrt{\frac{2(M_{\mathrm{i}}+\lambda_{\mathrm{c}} M_{\mathrm{uc}})}{\sigma_{\mathrm{c0}} t}} \frac{1}{h} \\ \eta_{\mathrm{b}} = \sqrt{\frac{2(M_{\mathrm{i}}+\lambda_{\mathrm{b}} M_{\mathrm{ub}})}{\sigma_{\mathrm{c0}} t}} \frac{1}{l} \end{cases}. \tag{14}$$

The friction coefficient between equivalent elastic plate and the contact surface is assumed as $\xi = 0.55$ [16], the ratio of material tension to compression strength is taken as $\alpha = 0.11$. Substituting ξ and α into the unified strength theory to determine using the formula (1), substituting equation (11) into equation (1), and the largest normal stress is given by

$$\sigma_{\mathrm{c0}} = -\frac{F + \sqrt{F^2 - \left(1 + \frac{(H\xi k)^2}{\alpha(1+b)}\right)\left(F^2 - \frac{H^2}{4\alpha^2}\right)}}{1 + (H\xi k)^{2} / [\alpha(1+b)]} \alpha f_{\mathrm{c}}\,, \tag{15}$$

$$\sigma_{\mathrm{b0}} = -\frac{F + \sqrt{F^2 - \left(1 + \frac{[H(\xi/k)]^2}{\alpha(1+b)}\right)\left(F^2 - \frac{H^2}{4\alpha^2}\right)}}{1 + (H\xi/k)^2/\alpha(1+b)}\alpha f_{\mathrm{c}}\,, \tag{16}$$

where, $F = \frac{1+b-\alpha}{2\alpha}$; $H = 1 + b + \alpha$; f_{c} is the compressive strength of composite materials.

In the actual situation, the material at the contact surface may not be the destroyed at the same time, Eqs. (**??**) and (**??**) give only the upper limit of stress the of contact surface, by comparing the predicate [13] (17) and (18), the normal stress can be obtained at the plastic state:

When

$$A_{\mathrm{c}} > A_{\mathrm{b}},\ \sigma_{\mathrm{c}} = \sigma_{\mathrm{c0}}\left(\frac{A_{\mathrm{c}}}{A_{\mathrm{b}}}\right)\ \sigma_{\mathrm{b}} = \sigma_{\mathrm{b0}}\,. \tag{17}$$

When

$$A_{\mathrm{c}} \le A_{\mathrm{b}},\ \sigma_{\mathrm{b}} = \sigma_{\mathrm{b0}}\left(\frac{A_{\mathrm{c}}}{A_{\mathrm{b}}}\right)\sigma_{\mathrm{c}} = \sigma_{\mathrm{c0}}\,, \tag{18}$$

$$\begin{cases} A_{\mathrm{c}} = k^2\sigma_{\mathrm{c0}}\eta_{\mathrm{c}}\left[1 - \eta_c - \xi k\right] \\ A_{\mathrm{b}} = \sigma_{\mathrm{b0}}\eta_{\mathrm{b}}\left[1 - \eta_{\mathrm{b}} - \xi k\right] \end{cases}. \tag{19}$$

4.2.3. Calculation steps

1. Calculate the maximum normal stress of contact surface by using Eqs. (15) and (16);
2. Calculate the ultimate bending moment on the cross-section;
3. Calculate the length of the contact area factors and by using Eq. (14);
4. Calculate the actual contact stresses and by using Eqs. (17) and (18);
5. Calculate the ultimate bearing capacity according to Eqs. (9) and (10).

5. The formula verification

This paper selected four different filled materials to validate the formula:

1. The aerated concrete for the ECW1 wall;
2. The fiber material filled adobe base for the ECW2 wall;
3. The fiber cement-based for the XLM1 wall;
4. The EPS of the regeneration lightweight aggregate for the XLM2 wall.

Using the low reversed cyclic loading, loading device is shown in Fig. 6. Vertical load is added on the distribution of beam by the jack, and then is passed on the rib column and frame column after the secondary distribution. Horizontal load is applied by the reaction wall.

The ultimate strength obtained from the test with different values are shown as Tab. 1.

Table 1. Comparisons of the ultimate strength obtained from the test with different values

Specimen			ECW1	ECW2	XLM1	XLM2
Vertical load (kN)			110	110	110	110
frame	size (mm)	frame-beam	50	50	50	50
		frame-column	100	100	100	100
	lenght×height (mm)		1400×1440	1400×1440	1400×1440	1400×1440
ribbed	size (mm)	ribbedd column	50	50	50	50
		ribbed-column	50	50	50	50
Elastic modulus (MPa)		concrete	2.55×10^4	2.55×10^4	2.55×10^4	2.55×10^4
		block	200	2000	5500	1245
Compressive strength (MPa)		concrete	27.6	27.6	27.6	27.6
		block	3.0	1.14	19.7	0.85
V_{exp} (kN)			81.6	74.6	133.9	83.2
V_k (kN)			88.2	83.9	149.4	87.2
$\frac{V_k - V_{exp}}{V_k}$			7.4 %	11.1 %	10.4 %	6.8 %

6. Conclusion

Based on the above analysis and discussion, we can conclude:

1. The effective compressive strength of the composite materials in the ultimate bearing capacity model of fibrous concrete wall is effective.

2. By using the unified strength theory and the whole diagonal strut model, the shear bearing capacity formula of fibrous concrete wall is derived and can satisfy the engineering requirements with a certain accuracy;

3. The shear bearing capacity formula can be applied for the shear bearing capacity calculations with different sizes, reinforcement and filled materials of the fibrous concrete wall.

References

[1] W. Huang, Q. Yao, Y. Zhang, Y. Wu: *Calculation on ultimate bearing capacity of multi-ribbed composite walls infilled with blocks.* China Civil Engineering Journal (2006), No. 3, paper 42.

[2] J. Ji, X. Han, Y. Zheng, J. Wang, Y. Chen, K. Yang: *Analysis of ultimate bearing capacity of coupled shear walls based on philosophy of capacity designw.* Earthquake Engineering and Engineering Vibration (2006), No. 4, 114–120.

[3] G. Chen, Y. Guo: *Ultimate shear-carrying capacity of steel plate shear wall with cross stiffeners.* Journal of Building Structures *25* (2004), No. 1, 71–78.

[4] S. H. Huang, X. J. Huang: *Computation of the ultimate bearing capacity of steel reinforced concrete low-rise shear walls with frame.* Journal of Southwest Jiaotong University *36* (2001), No. 4, 360–364.

[5] Q. Yao, W. Huang, J. Tian, Y. Ding: *Experimental analyses of mechanical characteristics and seismic performance of multi-ribbed panel wall.* Journal of Building Structures *25* (2004), No. 6, 67–74.

[6] M. H. Yu: *Twin-Shear Theory and Its Applications.* Science Press, Beijing, China (1998).

[7] D. J. Cook: *Expanded polystyrene concrete, Concrete Technology and Design: (1).* New Concrete Materials, Sur-rey University Press, London (1983), 41–69.

[8] M. H. Yu, L. N. HE: *A new model and theory on yield and failure of materials under complex stress state.* Mechanical Behariour of Materials-6, Pergamon Press, Oxford, UK *3*(1991), 841–846.

[9] W. Huang, Q. F. Yao, X. F. Zhang, G. Lu: *Calculation analysis on new type composite wall elastic lateral rigidity.* Earthquake Resistant Engineering and Retrofitting *27* (2005), No. 2, 1–7.

[10] D. J. Eshelby: *The determination of the elastic field of an ellipsoidal inclusion and related problems.* Proceedings of the Royal Society a Mathematical, Physical and Engineering Sciences (1957), Ser.No. A244, 376–3968.

[11] Zhou Fu, Fan Qun: *Composite Material Mechanical.* Higher Education Press (1991).

[12] Z. G. Xiong, S. F. Xu, J. Wei: *Masonry structures (2nd edition) National College of Civil Engineering textbook series(Chinese Edition).* Science Press, Beijing, China (2014).

[13] D. Hang, H. Chen, Z. Lu: *The investigation on analysis models of ultimate strength of reinforced concrete shear wall based on shear resistant mechanism.* Engineering Mechanics *24*(2007), No. 7, 134–139.

[14] H. L. Chen, D. C. Zhang, X. D. Zhang: *Modification on analysis models of ultimate strength of RC shear wall with opening.* Journal of Nanjing University of Technology *29*(2007), No. 2, 95–101.

[15] A. Saneinejad, B. Hobbs: *Inelastic design of infilled frames.* Journal of Structural Engineering *121* (1995), No. 4, 634–350.

[16] L. Yu, Y. Zhang, Q. Yao: *An experimental study on the load-bearing mechanism of elemental reinforced concrete frames under cyclic load.* China Civil Engineering Journal *40* (2007), No. 8, 47–53.

Received April 30, 2017